A Real-Time and Offline Quality Control Methodology for SeaSonde High-Frequency Radar Currents

SIMONE COSOLI AND GIORGIO BOLZON

Istituto Nazionale di Oceanografia e Geofisica Sperimentale, Sgonico, Trieste, Italy

ANDREA MAZZOLDI

Istituto di Scienze Marine, Consiglio Nazionale delle Ricerche, Sezione di Venezia, Venice, Italy

(Manuscript received 7 December 2011, in final form 4 May 2012)

ABSTRACT

A near-real-time and offline quality control methodology for SeaSonde systems is proposed. It is applied on radial current maps and is based on the determination of the signal-to-noise ratio (SNR) values of the Doppler lines that contribute to the hourly radial current at each range-bearing (R, θ) pair, under the assumption that SNR is a proxy for radar data quality. The retrieval of the sequence of Doppler lines is performed through a minimization procedure that takes advantage of the statistical descriptors output in the short-term radial maps. The separation of the contributing Doppler velocities into valid observations and anomalous velocities is based on their spectral quality factor and on a range-dependent noise threshold derived from statistics (average and standard deviation) of the signal amplitudes in the tails of the Doppler spectra. The final product of the quality control procedure is a radial current map, in which Doppler velocities are weighted by their SNR values and their spectral quality factors, and averaged to produce an output that is fully compatible with the proprietary software. This procedure is fast, despite the fact that a large number of combinations might be required during the retrieval of the Doppler lines, and effective, because it removes both evident spikes as well as Doppler velocities that are not clearly identified as anomalous velocities. In principle, this approach can be used to fill gaps in the radar coverage without the need for interpolation in time or space, proved that the Doppler velocities satisfy predetermined SNR constraints.

1. Introduction

The use of high-frequency (HF) radars for oceanographic studies constantly increased in the last years in many coastal regions of the United States and across Europe, resulting from their capabilities for mapping sea surface currents well beyond the horizon and over a wide variety of spatial and temporal scales. The ability of HF radars to provide near-real-time data also made them attractive outside the research community, so ocean radars were converted into valid tools for operational oceanography (Paduan et al. 2004).

As with any other instrumental measurement, HF radar currents are affected by errors resulting from hardware failures, external radiowave interferences, or poorly constrained inversion algorithms. Extensive comparisons with more conventional platforms performed either in different regions of the world's coastal oceans [such as current meters, drifters, or similar; see, e.g., Emery et al. (2004) and Paduan et al. (2006)], or with more advanced analysis tools (dePaolo and Terrill 2007; Laws et al. 2010) evidenced the general reliability of radar measurements, and provided upper bounds on the radar current measurement accuracy. Detailed investigations evidenced that the radar sampling strategy is potentially unable to resolve high-frequency finescale motions, and discrepancies with pointwise current meter records can be explained in terms of unresolved geophysical processes, such as horizontal current variability, Stokes and Ekman drift, and current-induced baroclinicity (Chapman and Graber 1997).

Nevertheless, despite the intrinsic differences introduced by the sampling strategies, it is generally well accepted that HF radars provide reliable estimates of surface current fields and waves.

Corresponding author address: Simone Cosoli, Istituto Nazionale di Oceanografia e Geofisica Sperimentale (OGS), Borgo Grotta Gigante 42/c, 34010 Sgonico, Trieste, Italy.
E-mail: scosoli@ogs.trieste.it

DOI: 10.1175/JTECH-D-11-00217.1

Parallel to the diffusion of HF radars, interest has increased in using sea surface current maps either for data assimilation into ocean circulation models, aimed at solving processes at a subgrid scale, or to provide corrections to model wind forcing (Oke et al. 2002; Breivik and Sætra 2001; Shulman et al. 2002; Paduan and Shulman 2004). Though limited to surface, HF radars in fact provide high-resolution real-time data on large observational grids at a relatively low cost and have the advantage of resolving rapidly varying current features that would require significant computational cost in ocean circulation models.

2. Quality control approaches

a. General approaches

While there is general agreement on the reliability of radar data for oceanographic applications, there is no agreement for quality assurance and quality control (QA–QC) procedures. Protocols for quality control and quality assurance of remotely sensed currents are neither well established nor standardized because of the different level of manipulation that radar data typically undergo (radial currents; surface current maps, merged from radial maps; wave data; particle tracks).

The majority of near-real-time QA–QC tests on radial currents for direction-finding (DF) systems, such as the SeaSonde radars [i.e., signal-to-noise ratio (SNR); first-order Bragg limits; metrics on the Multiple Signal Classification (MUSIC) direction-finding algorithm; single versus dual-angle solution (NOAA 2005)], require massive data manipulation on the proprietary software, thus often becoming either a time consuming or unpractical task to perform in near–real time. When dealing with commercial SeaSonde HF radars, some error metric is output in the hourly radial current map but, rather than expressing only measurement error, it provides a measure of the combined effect of instrumental error and the intrinsic temporal and spatial variability of the ocean motions during the measurement cycle.

Quality control procedures are more often applied to surface current maps, commonly derived from a least squares fit mapping of radial currents from two or more stations on a regular grid of arbitrary shape. In this case, QA–QC procedures rely on time domain checks that are based on either threshold values that vary on a regional scale or statistical moments of the surface velocity distributions and their first-order derivatives [see, e.g., Kovačević et al. (2004) for time domain despiking of sea surface current maps]. Procedures also exist that rely on more refined approaches (see, e.g., Goring and Nikora 2002).

One major limitation to this approach is the fact that it applies to the total current vectors, which are known to be affected by a geometrical dilution of precision (GDOP; Chapman and Graber 1997); that is, the inversion of radial maps to surface currents on a regular grid is influenced by geometrical constraints on the intersecting geometry beams, though the accuracy of the radial-to-vector mapping depends also on the number of radial velocities from each radar station [the geometrical dilution of statistical accuracy (GDOSA); see Barrick (2002), and on the unknown flow field (S. Cosoli and G. Bolzon 2012, unpublished manuscript)].

b. The signal-to-noise-ratio quality assurance–quality control procedure

In this work, an efficient and fast quality control procedure for the SeaSonde HF direction-finding radar systems is proposed that acts on radial velocity maps. It is based on the assumption that SNR is a valid proxy for data quality, which can be used to determine whether radial velocities at each range-bearing pair (R, θ) are either reliable current measurements or anomalous velocities to be removed prior to any subsequent calculation. The SNR QA–QC procedure determines the complete sequence of Doppler velocities (DVs) at each (R, θ), finds their SNR values from the Doppler spectra, and removes those data having SNR values that do not match predetermined constraints or quality criteria. Valid Doppler velocities are then weighted by their SNR values to define a quality-controlled radial velocity. The final output of the quality control procedure is a radial map that reproduces the standard output from the SeaSonde processing software, resulting in being fully compatible with other proprietary software tools.

Statistics of the quality-controlled radial velocities (i.e., SNR values) are also output in the radial map, with the aim of using them either as weights in the least squares current mapping or for diagnostic purposes.

The SNR QA–QC procedure makes use of an iterative approach to retrieve the unknown Doppler velocities. This choice is related to the processing scheme that the SeaSonde adopts to obtain radial maps. The hourly radial map is, in fact, derived from of a sequence of observations collected every 10 min (the "short-term radials" following the SeaSonde terminology). These, in turn, come from Doppler spectra that are collected and averaged over 15-min intervals. Short-term radials are averages of a number of Doppler bins that have been placed at each grid point, regardless of their SNR values.

Information on Doppler bins is no longer available after the short-term radial file has been created. Only their statistics are available, such as max/min values,

number of averaged Doppler lines, standard deviation or spatial uncertainty, and, after merging, standard deviation or temporal uncertainty. Thus, basically, it is an attempt to solve for an unknown sequence of Doppler velocities that originates the short-term radial currents at each grid point, based on the statistics of their distribution.

The proposed approach has many advantages. The method retrieves SNR values for each Doppler line despite the fact that they are not saved in the SeaSonde standard output. It provides a QA–QC assessment based on SNR and spectral quality factor (i.e., it accounts for interferences resulting from ship echoes during the acquisition process). A merging method that is different from the proprietary method is used, which takes advantage of all valid data and weights them by their SNR, giving preference to strong sea echoes and providing a more stable current estimate. Also, it solves for the problem of understanding which part of the signal powers are used in the MUSIC inversion, thus providing additional useful diagnostic tools.

The methodology is applied to standard range SeaSonde systems operating at 25 MHz, but it can be easily applied to any other SeaSonde HF radar and, in principle, to any other type of HF radar for oceanographic purposes. Similar methodologies and the use of SNR values as data quality proxy are, in fact, already applied to beam-forming (BF) phased-array systems (Parks et al. 2009). It operated in real-time and offline modes in the northern Adriatic Sea during the 2007–08 Northern Adriatic Sea Current Monitoring (NASCUM) initiative (Cosoli et al. 2012; Mihanović et al. 2011); it is currently operating on the 25-MHz SeaSonde systems in the northern Adriatic Sea. It was developed and made operational in real time for the SeaSonde Radial Suite 10, release 5, update 1, and can be easily adapted to any further software release.

There are many reasons to apply QA–QC procedures to the level of radial currents. Radials usually represent the lower level in the hierarchy of QA–QC protocols and are used to derive surface current maps. There is common agreement that errors at the level of radial currents need to be understood (Laws et al. 2010). The need for applying QA–QC protocols or procedures at the level of current vectors is minimized when good data are provided as input to the mapping procedure. High-quality radial currents can be assimilated into ocean circulation models, thus either limiting or reducing inconveniences related to GDOP or GDOSA [see, e.g., Barth et al. (2010) for assimilation of radial currents into numerical circulation models].

The manuscript is organized as follows. Section 3 introduces the fundamentals of the processing steps for standard 25-MHz SeaSonde HF radars, used here as a reference, which were installed in the northeastern Adriatic Sea in the second half of 2007. Section 4 describes the details of the proposed QA–QC approach, while section 5 discusses the assumptions of SNR as proxy for radar data quality and presents some results deriving from its application on real data. Finally, section 6 discusses the main results and findings.

3. Fundamentals of processing scheme for SeaSonde HF radars

HF radars measure surface currents by determining the Doppler shift of an electromagnetic wave after it is reflected from ocean waves with half the wavelength of the transmitted signal (Paduan and Graber 1997). The physical mechanism common to all types of HF radars for oceanographic purposes is known as Bragg scatter (Crombie 1955): the HF band signals are backscattered from ocean waves having half the wavelength of the transmitted radar wavelength. In the absence of ocean currents, the sea-echo signals identify two peaks symmetrically placed around the radar transmit frequency. When ocean currents are present, on the other hand, the two peaks are Doppler shifted and the magnitude of the shift is proportional to the sea surface currents over the near-surface depths that influence the particle motions of the Bragg waves (Stewart and Joy 1974).

The standard processing scheme for SeaSonde radars used for this study is based on the collection of sea-echo signals that originate from the reflection of a frequency-modulated interrupted continuous waveform (FMICW) signal transmitted in the 25-MHz-frequency band. Complex-valued voltage time series at the three antenna elements $[v_i(t), i = 1, 2, 3]$ are collected every 512 s; at a 2-Hz sampling rate, they correspond to a sampling interval of 4 min, 16 s.

The signal at the three antennas is range gated and fast Fourier transformed (FFT) to obtain raw spectra at the three antennas $[s_i(f), i = 1, 2, 3]$; then, raw spectra are cross multiplied to generate auto- and cross-spectra $[S_{ij}(f), i, j = 1, 2, 3]$, and ensemble averaged at blocks of three consecutive datasets to produce the so-called 10-min cross-spectra $(\langle S_{ij}(f)\rangle, i, j = 1, 2, 3)$.

Directional information of the radial currents is derived from the analysis of the 10-min cross-spectra. SeaSonde radars uses a DF algorithm known as MUSIC (Schmidt 1986) to derive the direction of arrival of $2(N - 1)$ signals for each Doppler line, with N being the number of antenna elements ($N = 3$) and the multiplying factor being related to the fact that Doppler spectra from either advancing or receding waves are processed independently.

The inversion of the 10-min cross-spectra produces a temporary output known as the short-term radial map (i.e., the 10-min radial or short-term radial). Every hour, a sequence of up to seven consecutive 10-min maps collected around the cardinal hour is merged to produce a surface current map containing the surface current for each radar station over the radar footprint.

4. The SNR QA–QC methodology

In this section the proposed quality control procedure is described. The first step is the determination of the sequence of Doppler lines that define the hourly radial velocity in the radar domain. A quality threshold is then introduced, based on the SNR values at the monopole, the intrinsic variability of the signal level at the tails of the Doppler spectra, and the spectral quality factor output in the SeaSonde Doppler spectra files. This threshold is used to discriminate between valid and suspicious data. Finally, a modified merging method is introduced, which weights the valid data by their SNR and spectral quality values and provides the final hourly radial map.

a. Determination of the Doppler lines

The key step in the SNR QA–QC procedure is the determination of the sequence of Doppler lines that defines the hourly radial velocity at each range-bearing (R, θ) pair. This is achieved with the analysis of the sequence of 10-min short-term radials maps, which are the output of the inversion of the 15-min-averaged Doppler spectra (section 3).

For each (R, θ) pair, the short-term radial maps store the coordinates (longitudes and latitudes), the distance to the antenna (east and north components), the range cell (RC) and the bearing, and the average radial velocity and its direction, along with the statistics of the ensemble of Doppler lines that are averaged to produce the 10-min radial current.

The statistics include the extremes (velocity maximum and minimum), the standard deviation ("spatial quality"), and the dimension ("quality DV count") of the ensemble of Doppler lines that contribute to the 10-min radial currents. This set of statistical descriptors is at the basis of the SNR QA–QC procedure, because it allows for an unambiguous retrieval of the sequence of Doppler velocities.

When DV count is less than three the sequence of Doppler lines is easily retrieved. In the simplest case (DV count = 1), the unknown Doppler line matches both the average value and the velocity extremes. When DV count = 2, the two unknown Doppler lines coincide with the given velocity extremes. When DV count $\geq$ 3, the sequence of unknown Doppler lines is determined through an iterative procedure that minimizes a cost function of the spatial quality (i.e., the standard deviation) and the average radial current.

The iterative procedure first determines the candidate velocities in the minimum–maximum interval at the given Doppler resolution, and then cycles through their possible combinations and finds the sequence that minimizes the cost function given the required number of unknown Doppler lines. Convergence is reached and the iterative procedure ends when the distance of the solution provided by the ensemble of Doppler lines from the given statistical descriptors is smaller than a preset tolerance, or a maximum number of iterations is reached. Once the sequence of unknown Doppler lines is obtained, each value is associated with the corresponding SNR value by matching the SeaSonde Doppler spectrum file associated with the 10-min radial map.

Because it was intended to operate in real time, the iterative procedure is currently implemented to solve a maximum of 14 unknown Doppler lines at each bearing, the maximum number of iterations set to 10^{20}. In the case of failure in convergence resulting from either a larger number of Doppler velocities or a larger number of iterations, all Doppler lines for this (R, θ) are set to zero and excluded from the subsequent merging. SNR values of the resolved Doppler lines are extracted from the monopole Doppler spectrum because of its omnidirectional pattern and the fact that it stores useful information, such as for interferences or ship echoes.

b. Definition of SNR QA–QC criteria

As anticipated in section 3, radar backscatter data recorded by an operational SeaSonde system are complex-valued voltages [$v_i(t)$, i = 1, 2, 3 for antenna loops 1, 2, and the vertical monopole, respectively] at the three antenna elements. After range gating, FFT processing, and averaging, they are stored in Doppler spectra data files along with the self- and cross-spectra, and are complemented with a spectral quality index (QI) in the range [−1; 1], which accounts for external interferences for each Doppler velocity at every range cell.

SNR values of the Doppler velocities are defined as the spectral height of each line with respect to some noise level. Let i (i = 1, 2, 3) be the index of the antenna element to which the Doppler spectrum refers, let j (j = 1: 512) be the index of the Doppler velocities in the Doppler spectrum, let k (k = 1: 31) be the range cell index, and let S_{ijk} be the spectral amplitude of the jth Doppler velocity for kth range cell at the ith antenna element. Spectral amplitudes are first converted to dBm as

$$S_{ijk} = 10 \log_{10}[\text{abs}(S_{ijk})] - 40.0 + 5.8,$$

where +5.8 represents an adjustment factor to signal processing loss and −40.0 is an adjustment for receiver gain (CODAR 2005). Note that spectral amplitudes need to be absolute to avoid negative values at antenna 3 (a flag for external interferences). A noise floor level (NF_{ik}) is computed separately for each kth range cell at each ith antenna element by averaging the spectral amplitudes of the Doppler velocities in the tails of the spectra (from approximately −1 to −0.6 Hz, and from +0.6 to 1 Hz). Then, the signal-to-noise ratio (SNR_{ijk}) for the jth Doppler line at the kth range cell of the ith antenna, expressed in decibels, is given by $SNR_{ijk} = S_{ijk} - NF_{jk}$. As anticipated in the previous section, SNR values for the resolved Doppler lines are referred to the monopole antenna ($i = 3$) because of its omnidirectional sensitivity pattern and the fact that it both defines the amplitude of the first-order Bragg region and stores information on interferences from external sources.

The proposed SNR QA–QC methodology, in addition to the noise floor level NF_{jk}, defines a dynamic, range-dependent threshold that accounts for signal attenuation over range and sets more severe constraints on spectral amplitude of the Doppler velocity. It is defined as

$$\text{quality\_threshold} = NF_{ik} + n\sigma(S_{ijk}),$$

where NF_{ik} is the noise floor level for the kth range cell at the ith antenna, $\sigma(S_{ijk})$ is the standard deviation of the signal spectral amplitude in the region where noise level is computed, and n is a multiplying factor (set to $n = 2$ for range cells < 20, and $n = 3$ for range cells > 21). Any jth Doppler velocity having an SNR $<$ noise threshold is considered noise and is removed from the sequence before the averaging process. Similarly, any Doppler velocity a having spectral quality factor $Q_j <$ 0.9 is removed before averaging.

The standard deviation term is meant to account for the intrinsic variability of signal amplitude in the tails of the spectra where the noise is computed; the multiplier factor is intended to account for signal propagation loss with range, which determines lower echo intensities at distant range cells and increases the possibility of false signal detection and lower accuracy in bearing estimate. In other terms, Doppler velocities at distant range cells are required to satisfy more severe SNR constraints to be included in the radial current output.

After the SNR-based checks, the hourly output is obtained as the average of the valid Doppler velocities, weighted by their SNR and spectral quality factors (Q_i),

$$v_i(R,\theta) = \frac{\sum_i v_i(\text{snr}_i)Q_i}{\sum_i (\text{snr}_i)Q_i}.$$

Finally, a consistency check is performed at each location aimed at removing correct radial velocities at the wrong angular sectors. The consistency check recursively compares the hourly radial velocity with the average radial currents from surrounding locations (±5° in bearing, and ±1 range cell in range), deletes velocities that have large velocity gradients, and stops when the offset is lower than a preset tolerance.

The final output of the SNR QA–QC procedure is a radial map, in which the structure of the original file (header, longitude, latitude, velocity components, quality flags, range to the antenna, speed, and bearing) is preserved to make it fully compatible with the SeaSonde proprietary software. The only modification provided by the SNR QA–QC approach to the radial map file is that the cumulative SNR amplitude of each radial velocity is output at each (R, θ) pair instead of the "temporal quality flag" as a measure of data reliability.

5. The SNR QA–QC methodology at work

In the following sections it is shown that SNR can be considered as a valid proxy for radar data quality; then, examples at selected locations in the radar coverage are given to prove the SNR QA–QC method's effectiveness in removing outliers.

The first task is accomplished with the analysis of the velocity differences between moored current data and coincident radar radial currents for the closest radar grid point, in relation to their SNR values. The outlier removal capabilities are shown against a clear spike introduced by low SNR-valued Doppler velocities [section 5a(1)]; a more complicated example is shown in the following section [section 5b(2)].

The SeaSonde radars used to collect data used in this work were set up in the northern Adriatic Sea as part of the NASCUM INTERREG initiative between Italy and Croatia, conducted under the sponsorship of the European Union (Cosoli et al. 2012; Mihanović et al. 2011). They operated in the 25-MHz band, with a 1.5-km resolution in range and 5° resolution in angle, and used the ideal antenna beam patterns with phases and amplitudes corrected after antenna pattern measurements (Table 1). Raw Doppler spectra were collected every 4 min (256 s), ensuring a Doppler velocity resolution of $\Delta v = (\lambda_r/2T) = (c/2n\Delta T f_r)$, approximately 2.2–2.3 cm s^{-1} at the radar frequency f_r, sampling period T, 512-point spectral resolution, and 2-Hz sample rate. Subsurface currents were collected using a downward-looking

TABLE 1. Characteristics of the SeaSonde HF radars installed in the northern Adriatic Sea for the period July 2007–December 2008. The site names are given, along with the coordinates, operating frequencies, velocity resolution (cm s^{-1}), and operating period.

Radar site (radar site code)	Coordinates	Operating frequency (MHz)	Transmit bandwidth (kHz)	Doppler velocity resolution (cm s^{-1})	Operating period
Rt Zub (PZUB)	45°17′54″N, 13°34′08″E	25.6	100.708	2.28	July 2007–December 2008
Savudrija (SVDR)	45°29′23″N, 13°29′27″E	24.9	100.708	2.35	July 2007–December 2008
Punta Tagliamento (BBIN)	45°38′11″N, 13°05′51″E	24.7	100.708	2.37	December 2007–August 2008
Punta Sabbioni (PSAB)	45°25′22″N, 12°26′12″E	25.3	75.073	2.31	March 2008–August 2008

1000-kHz Aquadopp profiler (AQP) on the MAMBO-4 (also, mogs4) oceanographic buoy, located outside the Trieste Gulf along the Punta Tagliamento (BBIN)–Savudrija (SVDR) baseline (43°33.95′N, 13°14.86′E; Fig. 1). The current meter provided measurement with a temporal resolution of 5 min and a vertical resolution of 1 m, with the level closest to surface set at a nominal depth of 1.55 m.

Given that SNR QA–QC is capable of retrieving the sequence of Doppler lines and corresponding SNR values for each hourly radial velocity in the radar coverage, storing them for the radial sector closest to the current meter mooring is a relatively easy task. Time series of radar radial currents and corresponding SNR values can then be used to interpret differences with mooring data in terms of SNR values. Though there are many sources that contribute to differences [instrumental errors and bearing offsets, different sampling strategies, and unresolved geophysical variability; see, e.g., Chapman et al. (1997)], this analysis shows the potential contribution of SNR to radar data reliability.

To provide statistical significance to the analysis, the comparison is carried out with the 10-min radial currents (average value of the Doppler velocities) and corresponding SNR values at the 10-min time step. Moored currents similarly are averaged at 10-min intervals to match, as close as possible, the 10-min radar data, and projected onto the direction of the radar site. Comparisons are performed for BBIN–mogs4 (17 December 2007–13 March 2008), and for SVDR–mogs4 and Rt Zub

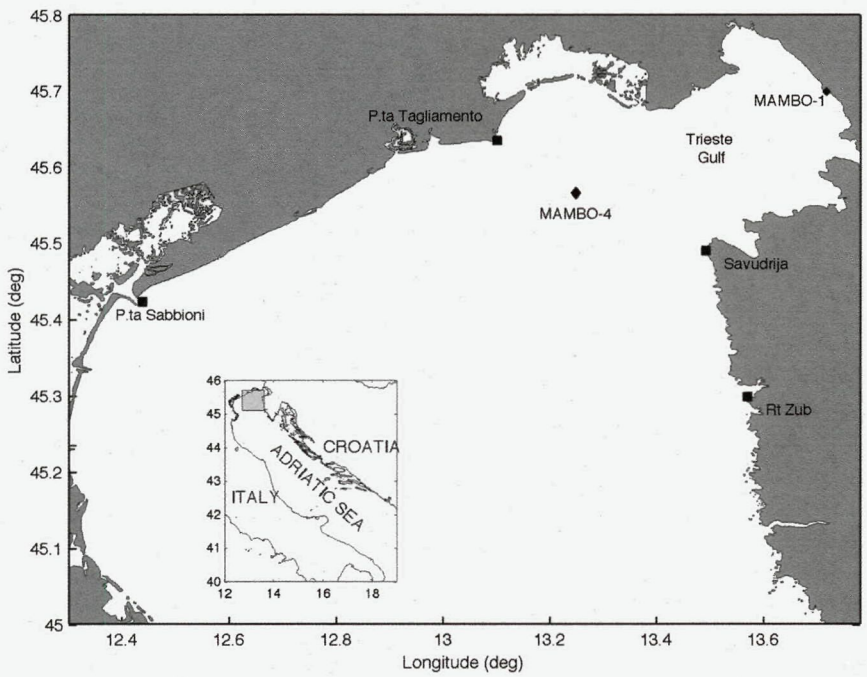

FIG. 1. The study area, in the northeastern corner of the Adriatic Sea, with the locations of the radar stations used in this study (Rt Zub, Savudrija to the east, and Punta Tagliamento to the north), and the locations of the MAMBO buoys are shown. The MAMBO-4 buoy was equipped with a current profiler and provided data for a ground truth validation of the quality control procedure.

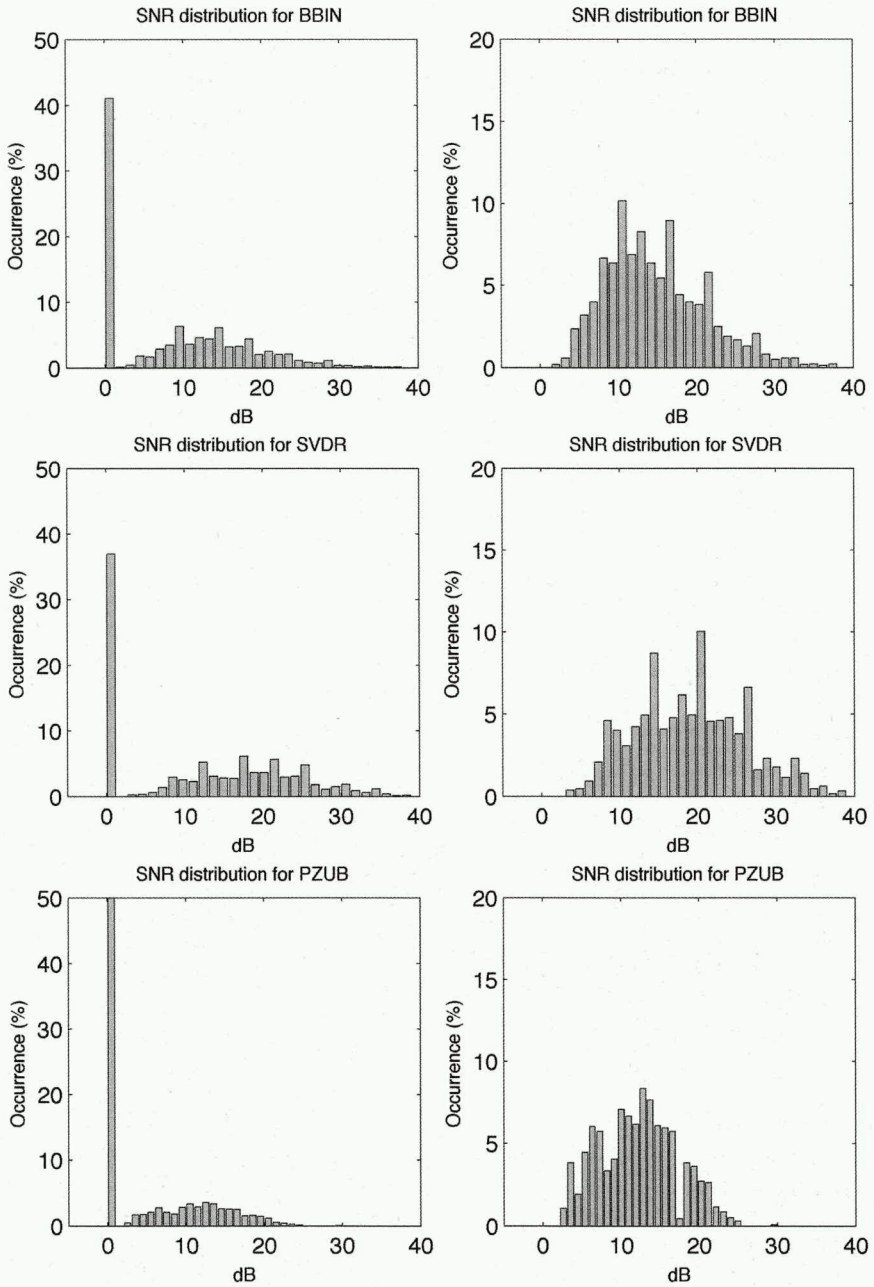

FIG. 2. Distributions of SNR values for the 10-min radar velocities at the (top) BBIN, (middle) SVDR, and (bottom) PZUB radar sites, used for the radar to current meter comparison. Histograms refer to (left) radar velocities with all SNR values and (right) radar velocities with SNR > 0 dB.

(PZUB)–mogs4 (1 February 2008–13 March 2008 and 30 January 2008–13 March 2008, respectively) for the radar grid point that best matches the current meter location.

a. SNR as a proxy for radar data quality

Statistics of the SNR distributions for the 10-min radar currents coincident with current meter data reveal a significant presence of low SNR values (Fig. 2; note that SNR < 1 dB are set to SNR = 0 dB by the SNR QA–QC round-off approximation): they represent more than 41% of the radar SNR values at BBIN, about 37% of SNR values at SVDR, and more than 57% of the 10-min SNR values at PZUB. When low SNR–valued currents (i.e., requiring SNR to be above 1 dB) are excluded from the statistics, the resulting distributions for the three sites present a more Gaussian-like shape with SNR values as

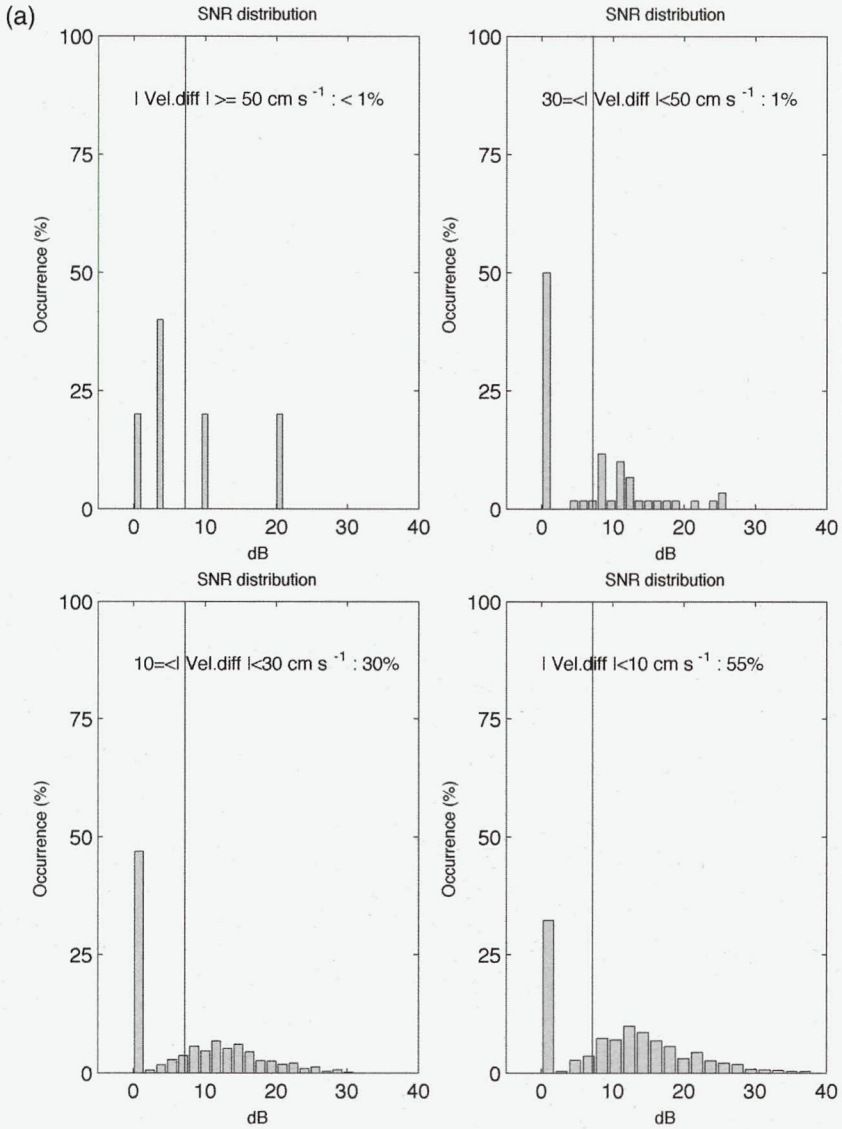

FIG. 3. (a) Distributions of the SNR values (dB) of the 10-min radar velocities as a function of velocity difference (cm s^{-1}) classes ($|\Delta_{vel}| > 50$ cm s^{-1}, 50 cm $s^{-1} < |\Delta_{vel}| \leq 30$ cm s^{-1}, 30 cm $s^{-1} < |\Delta_{vel}| \leq 10$ cm s^{-1}, and $|\Delta_{vel}| < 10$ cm s^{-1}) for the BBIN radar site. Velocity differences are obtained for radar radial currents at the sector closest to the current meter location. The time period for the comparison extends from 17 Dec 2007 to 13 Mar 2008. The percent occurrence for radar currents in each SNR class is given in the plot. The vertical line represents the SNR threshold that would have been required in the SNR QA–QC approach at this radar range cell. (b) Distributions of the SNR (dB) values of the 10-min radar velocities at the SVDR site as a function of velocity difference (cm s^{-1}) classes ($|\Delta_{vel}| >$ 50 cm s^{-1}, 50 cm $s^{-1} < |\Delta_{vel}| \leq 30$ cm s^{-1}, 30 cm $s^{-1} < |\Delta_{vel}| \leq 10$ cm s^{-1}, and $|\Delta_{vel}| <$ 10 cm s^{-1}). Velocity differences are obtained for radar radial currents at the sector closest to the current meter location. The time period for the comparison extends from 1 Feb 2008 to 13 Mar 2008. The percent occurrence for radar currents in each SNR class is given in the plot. The vertical line represents the SNR threshold that would have been required in the SNR QA–QC approach at this radar range cell. (c) Distributions of the SNR values (dB) of the 10-min radar velocities for PZUB–mogs4 pair as a function of velocity difference (cm s^{-1}) classes ($|\Delta_{vel}| > 50$ cm s^{-1}, 50 cm $s^{-1} < |\Delta_{vel}| <= 30$ cm s^{-1}, 30 cm $s^{-1} < |\Delta_{vel}| <= 10$ cm s^{-1}, and $|\Delta_{vel}| < 10$ cm s^{-1}). Velocity differences are obtained for radar radial currents at the sector closest to the current meter location. The time period for the comparison extends from 30 Jan 2008 to 13 Mar 2008. The percent occurrence for radar currents in each SNR class is given in the plot. The vertical line represents the SNR threshold that would have been required in the SNR QA–QC approach at this radar range cell.

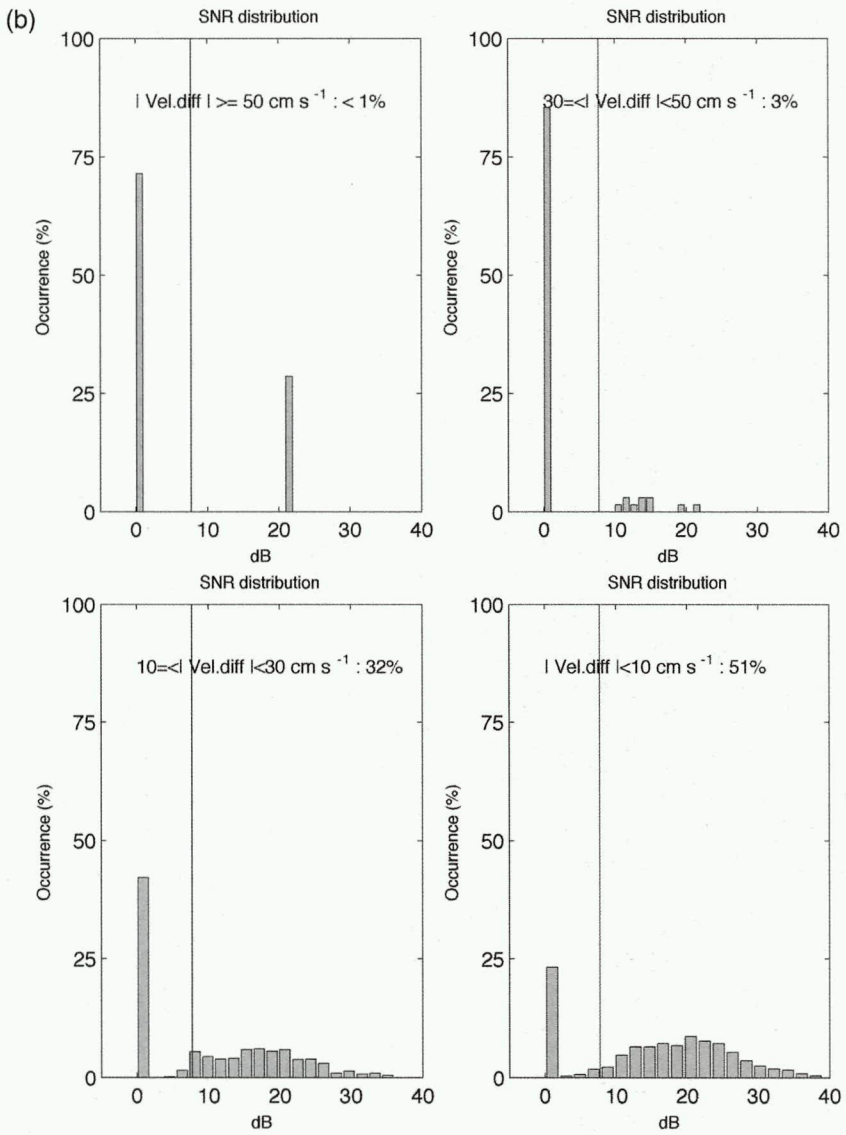

FIG. 3. (*Continued*)

high as 40 dB (BBIN and SVDR), and up to 30 dB (at PZUB site).

Distributions of velocity differences as function of SNR classes (SNR = 0 dB, SNR > 0 dB, SNR > 0 dB and SNR ≤ 6 dB, SNR > 6 dB and SNR ≤ 10 dB, SNR > 10 dB and SNR ≤ 20 dB, and SNR > 20 dB) show that the largest velocity differences are, in general, associated with poorly SNR-constrained radar currents. For radar currents having 0-dB SNR, differences are found in the range [37.7; −62.2] cm s^{-1} (BBIN), [82.7; −46.2] cm s^{-1} (SVDR), and [70.2; −23.8] (PZUB), though their 2.5th, 50th, and 97.5th percentiles are, respectively, (−20.2, 4.2, 26.6) cm s^{-1}, (−34.3, 1.8, 12.2) cm s^{-1}, and (−13.4, 4.1, 51.3) cm s^{-1}. Excluding near-zero-valued radar currents determines a general improvement in the comparison statistics, because both the extremes and the percentiles of the distributions tend to reduce in magnitude and cluster around zero as SNR values increase. For the SVDR–mogs4 pair, the extremes of the velocity differences decrease, respectively, to (56.9, −30.8) cm s^{-1} with the 2.5th, 50th, and 97.5th percentiles, decreasing to (−16.4, 2.0, 24.5) cm s^{-1}. For the PZUB–mogs4 pair, removing the low SNR–valued radar velocities also transforms the bimodal distribution found with the radial currents before the SNR QA–QC analysis into a Gaussian-shaped distribution.

Similarly, the distributions of the SNR values of radar currents for classes of velocity differences ($|\Delta_{vel}| \geq 50$ cm s^{-1}, 50 cm $s^{-1} < |\Delta_{vel}| \leq 30$ cm s^{-1}, 30 cm $s^{-1} < |\Delta_{vel}| \leq 10$ cm s^{-1}, and $|\Delta_{vel}| < 10$ cm s^{-1}) for the three

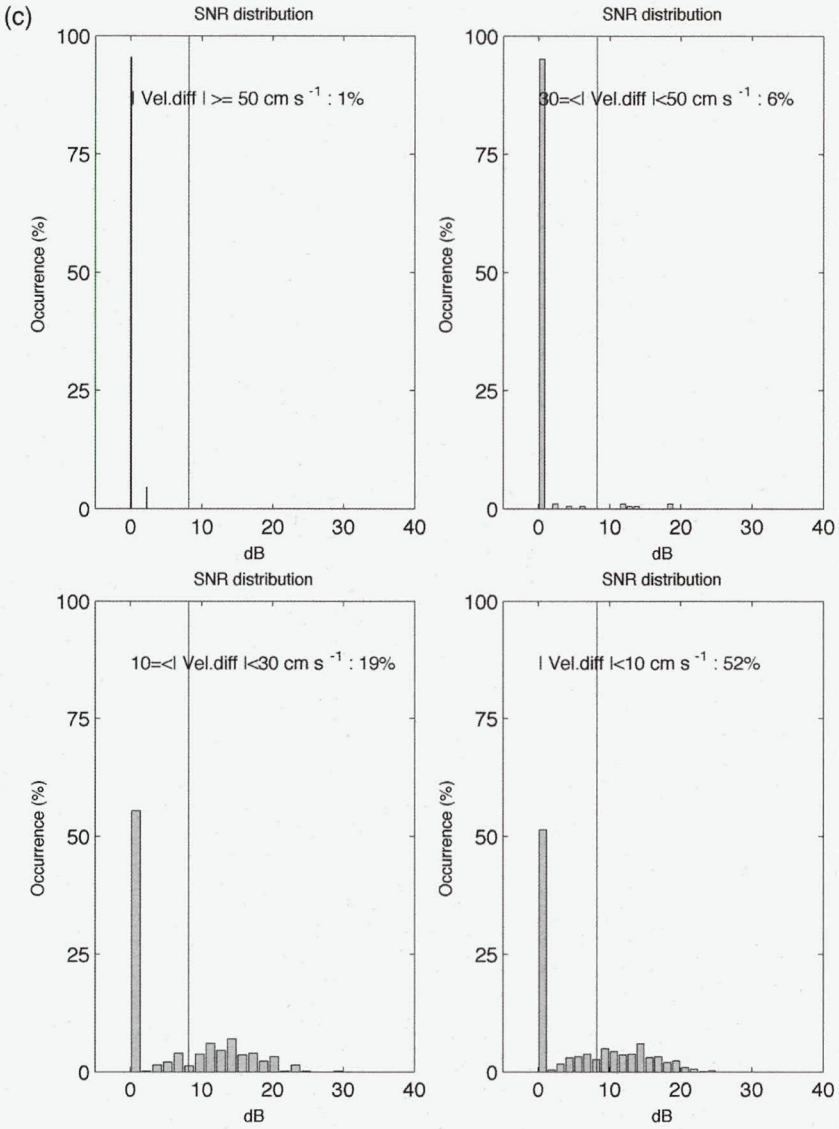

FIG. 3. (*Continued*)

comparison pairs (Fig. 3) show that velocity differences strongly depend on SNR. For the PZUB–mogs4 pair, the great majority of velocity differences for all classes are related with radar currents having SNR = 0 dB (99% for $|\Delta_{vel}| \geq 50$ cm s^{-1} and 50 cm s^{-1} $< |\Delta_{vel}| \leq$ 30 cm s^{-1}, 60% for 30 cm s^{-1} $< |\Delta_{vel}| \leq 10$ cm s^{-1}, and about 51% for $|\Delta_{vel}| < 10$ cm s^{-1}). These percentages are somewhat lower for the two other radar sites (about 75% for $|\Delta_{vel}| \geq 50$ cm s^{-1}, about 80% for 50 cm s^{-1} $< |\Delta_{vel}| \leq 30$ cm s^{-1}, 40% for 30 cm s^{-1} $< |\Delta_{vel}| \leq 10$ cm s^{-1}, and 25% for the SVDR–mogs4 pair; about 22%, 50%, 48%, and about 32% for the same velocity difference classes at the BBIN site), but in general reflect the same trend showing large differences associated with poorly constrained radar velocities.

Although somewhat infrequent, large differences may also appear with high SNR values (SNR > 10 dB and SNR > 20 dB). Their presence is presumably due to ambiguities in the determination of their direction of arrival; that is, they identify "true" Doppler velocities with incorrect bearing estimates, and are removed from the final output by the consistency check. Similarly, the SNR QA–QC approach would have excluded almost all of the low SNR velocities, because it requires a minimum SNR threshold of 7.2, 7.7, and 8.2 dB for BBIN, SVDR, and PZUB radars (range cells 9, 14, and 26), respectively.

b. *The SNR QA–QC methodology at work*

To evaluate the capabilities of the SNR QA–QC approach, the method is tested on the hourly radial map

TABLE 2. Summary of the iterative procedure for the radial current at range cell 30, bearing 0° (NCW) at1500 UTC 2 Jun. DV count is the number of Doppler lines that define the radial velocity. The Bragg peak from which the Doppler velocity originates is indicated (L: left-hand side, R: right-hand side), along with the SNR values at the three antennas (dB) and the quality factor.

Cross-spectra file	Bearing	Range cell	DV count	Radial velocity (cm s^{-1})	Doppler velocity	Bragg peak	SNR1 (dB)	SNR2 (dB)	SNR3 (dB)	Quality factor	Included
CSS_PZUB_08_06_02_1430.cs4	0	30	2	−60.1	−61.25	L	−2.85	0.51	0.14	1.0	No
					−58.96	L	−0.6	−1.22	1.04	1.0	No
CSS_PZUB_08_06_02_1440.cs4	0	30	1	−81.93	−81.93	L	0.12	−0.48	2.03	1.0	No

collected at 1500 UTC 2 June 2008 at the PZUB radar station.

1) TEST CASE: THE EVIDENT SPIKE

Radial current at 1500 UTC 2 June 2008, at RC 30, and bearing (θ) 0° measured clockwise from north (NCW) exceeds 70 cm s^{-1} in magnitude and is not consistent with radial velocities at surrounding locations. At this range from the antenna, the SNR QA–QC method requires an SNR threshold of 9 dB to include a Doppler line in the averaging process.

The radial velocity at this location is derived from observations at 1430 and 1440 UTC. As for the first short-term radial velocity map, the SNR QA–QC inversion retrieves two Doppler lines (−61.25 and −58.96 cm s^{-1}) from the left-hand Bragg peak. Their SNR values at the monopole (Table 2) are, respectively, 0.14 and 1.04 dB, with SNR values at the two loops being close to zero or negative. At 1440 UTC, only one Doppler line (−81.93 cm s^{-1}; the left-hand Bragg peak) defines the radial current magnitude. Its SNR value at the monopole is positive (2.03 dB), being negative at loop 1 and near-zero valued at loop 2.

Despite their good spectral quality (QF = 1), Doppler lines that contribute to the radial velocity at this location do not match the desired SNR QA–QC standards and are rejected from the subsequent calculations.

2) TEST CASE: THE HIDDEN SPIKE

Radial current at 1500 UTC 2 June 2008, RC 28, and bearing (θ) 345° (NCW) barely exceeds −22 cm s^{-1} in magnitude and appears to be consistent with radial velocities at the surrounding locations. The hourly radial velocity at this location is obtained from the 10-min radial maps at 1430, 1500, 1510, 1520, and 1530 UTC (Table 3). As for the previous case, at this range, the SNR QA–QC method requires an SNR threshold of 9 dB for each Doppler line to be included in the averaging process.

Two Doppler lines (−60.5 and −1.5 cm s^{-1}) from the right- and left-hand Bragg peaks define the 10-min radial current at 1430 UTC. None of the resolved Doppler lines satisfy the SNR QA–QC threshold, with the first Doppler velocity having SNR values in the range (−1.3; 1.4 dB) at the three antennas, and despite the higher SNR values of the second Doppler line (SNR values in the range 7.4–8.9 dB).

Similarly, two Doppler lines (−42.12 and 9.96 cm s^{-1}) from the right- and left-hand-side Bragg peaks, respectively, define the radial current at 1500 UTC. Of the two values, only the second (9.96 cm s^{-1}) meets the SNR QA–QC criteria (SNR values at the three channels are in the range 6.6–9.3 dB) while the second Doppler line was rejected.

TABLE 3. Summary of the iterative procedure for the radial current at range cell 28, bearing 345° (NCW) at 1500 UTC 2 Jun. DV count is the number of Doppler lines that define the radial velocity. The Bragg peak from which the Doppler velocity originates is indicated (L: left-hand side, R: right-hand side), along with the SNR values at the three antennas (dB) and the quality factor.

Cross-spectra file	Bearing	Range cell	DV count	Radial velocity (cm s^{-1})	Doppler velocity	Bragg peak	SNR1 (dB)	SNR2 (dB)	SNR3 (dB)	Quality factor	Included
CSS_PZUB_08_06_02_1430.cs4	345	28	2	−31.01	−60.5	R	1.37	0.28	−1.29	1	No
					−1.53	L	7.4	8.91	8.09	1	No
CSS_PZUB_08_06_02_1500.cs4	345	28	2	−16.08	−42.12	R	−4.95	0.55	−1.82	1	No
					9.96	L	6.64	7.94	9.03	1	Yes
CSS_PZUB_08_06_02_1510.cs4	345	28	1	6.12	6.12	R	14.38	14.04	17.77	1	Yes
CSS_PZUB_08_06_02_1520.cs4	345	28	1	−22.2	−22.2	L	4.33	−2.85	1.31	1	No
CSS_PZUB_08_06_02_1530.cs4	345	28	1	6.12	6.12	L	1.86	0.46	−1.4	1	No

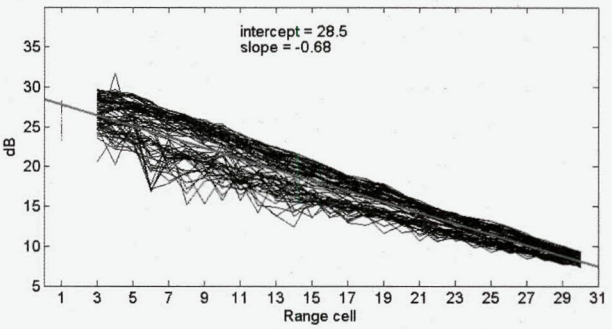

FIG. 4. SNR decrease over range cell and bearing angle for the period of June 2008 at the PZUB radar site. The linear fit for the average SNR decay over range cell is shown (thick gray line). Intercept and slope of the regression line are shown on the plot.

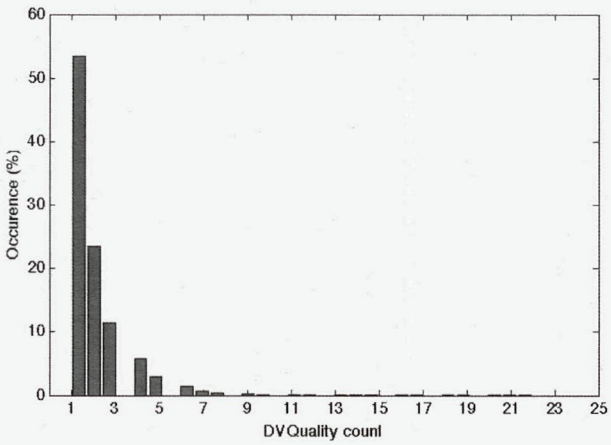

FIG. 5. Distribution of the DV count (i.e., number of Doppler lines) that are averaged to define the 10-min (short term) radial maps for PZUB radar station.

One Doppler line identifies the corresponding radial currents at 1510, 1520, and 1530 UTC (6.12 cm s^{-1}, SNR > 14 dB at the three antennas at 1510 UTC; −22.2 cm s^{-1}, SNR values in the range −2.8–4.3 dB at 1520 UTC; −24.5 cm s^{-1}, SNR in the range −1.4–1.8 at 1530 UTC, respectively). Only the radial current at 1510 UTC meets the SNR quality threshold, and the remaining values are rejected from the subsequent computations.

The standard merging approach computes the hourly average as the median value of the sequence of 10-min average currents, resulting in a radial current of −22.2 cm s^{-1}. When the valid Doppler lines are averaged accordingly to their SNR values, the resulting radial current has a magnitude of +7 cm s^{-1}.

6. Discussion

In this work, a methodology for real-time quality control of SeaSonde radial currents is described, which acts at the level of Doppler velocities and uses the signal-to-noise ratio (SNR) and spectral quality factor (Q) to discriminate between valid and questionable observations. In principle, the method can also be extended to phased-array systems for which the determination of the SNR of each Doppler line is more straightforward. Methodologies similar to what was proposed for the computation of the average radial velocity at each (R, θ) pair in fact exist, where SNR weighting acts as a "center of gravity" technique that gives preference to strong sea echoes providing a more stable current estimate (Barth et al. 2010).

It is an inverse approach that, rather than processing the cross-spectra files through an independent implementation of the MUSIC direction-finding algorithm, determines the unknown sequence of Doppler lines from the statistics of their distributions at each range and bearing in the short-term 10-min maps. This is performed through an iterative procedure that requires the minimization of a cost function of the available statistical moments. The reliability of the resolved Doppler lines is determined by its spectral amplitude at the monopole, relatively to the noise level and its variability, and their spectral quality factors Q, which is the signal-to-noise ratio weighted for by the quality of each Doppler velocity. The noise variability is accounted for by the standard deviation of the signal level in the region of the Doppler spectra where the noise-floor level is computed. This term acts as a dynamically set threshold that imposes more severe constraints on the SNR values of the resolved Doppler lines. The proposed quality threshold then constitutes a conservative choice in the sense that it would allow only for the strongest signals to be inverted through MUSIC with a reasonable accuracy of the bearing estimate. The choice of a step function with $n = 2$ for RC < 20 and $n = 3$ for RC > 21 is arbitrary, and a linear decrease with range would probably be more appropriate (as suggested by Fig. 4). This choice is based on the assumption that the probability of false-alarm detections (i.e., echoes that barely meet the above-the-noise detection threshold are processed to velocity) increases at large ranges to the antenna, resulting from the signal propagation loss with range. Analyses of the variability of spectral amplitudes at the Doppler spectra tails of distant range cells (not provided here) show that the σ term in the equation is comparable with amplitudes of the resolved Doppler lines in the Bragg region. Thus, setting $n = 3$ gives lower probability that the processed line is noise rather than signal. The choice of the vertical monopole antenna as a reference for SNR calculations is based on its omnidirectional properties

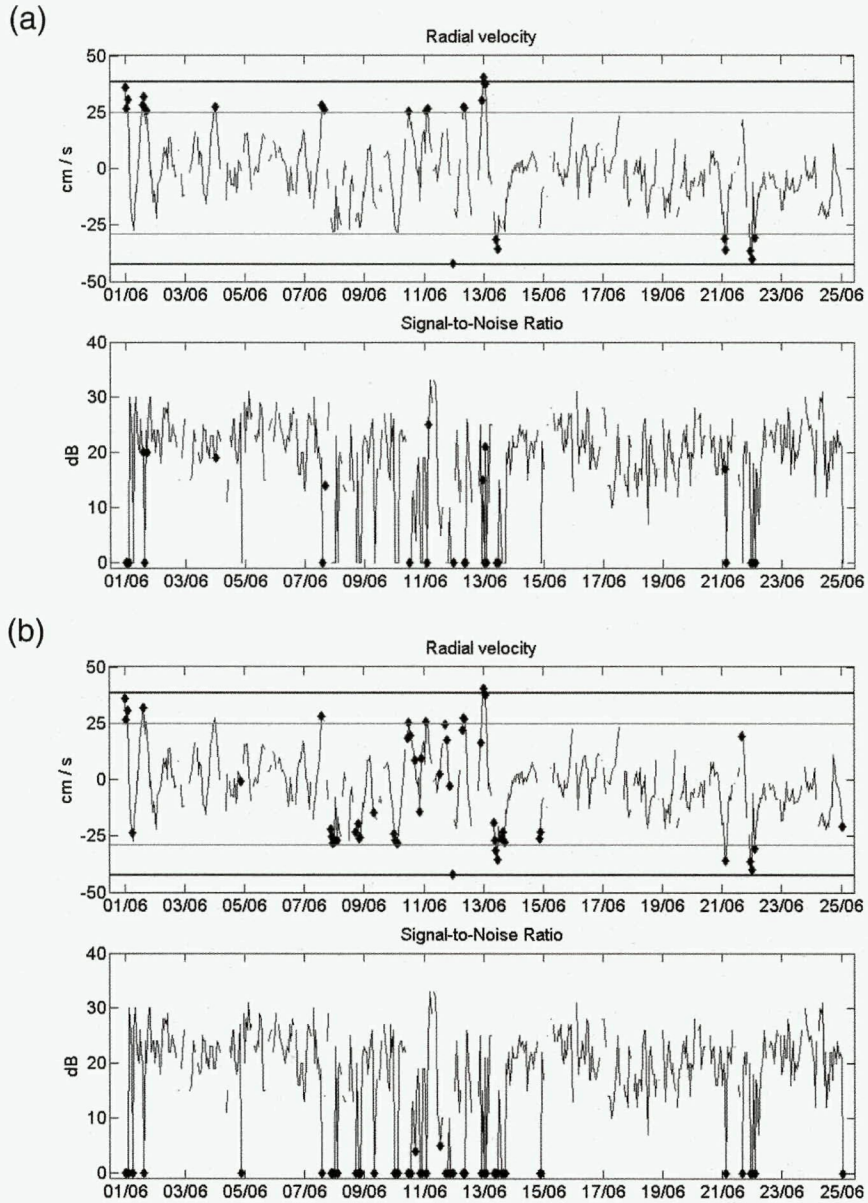

FIG. 6. (a) (top) Time series of radial current velocity with error bounds set as 2 times (thick gray lines) and 3 times (black thin lines) its standard deviation. Radial velocities are identified (black squares), with deviation from the median value larger than 2 or 3 times the standard deviation (MAD > 2 SD or MAD > 3 SD, respectively). (bottom) The time series of SNR values associated with the radial currents. The SNR values of radial velocities above having MAD > 2 SD or MAD > 3 SD are identified (black boxes). (b) (top) Time series of radial current with error bounds set as 2 times (thick gray lines) and 3 times (black thin lines) its standard deviation. Radial velocities having SNR values below the 6-dB threshold are identified (black squares). (bottom) The time series of SNR values associated to the radial currents are shown. SNR values below the 6-dB threshold are identified (black boxes).

and its use in the proprietary software to set the width of the first-order Bragg region.

The output of the SNR QA–QC procedure is a radial current map in which the structure of the original data file (header, longitude, latitude, velocity components, quality flags, range to the antenna, speed, and bearing) is preserved to guarantee its compatibility with the proprietary software.

The procedure is fast and effective, because it requires less than 2.5 s on a 1.33-GHz Power PC G4 Macintosh

TABLE 4. First-order settings adopted in the PZUB radar site, compared to default SeaSonde values. Noise factor identifies the lower threshold for Doppler velocities; smearing width is the amplitude of the running-average filter used to discriminate between first and second order; "nsec" and "fdown" determine the nulls between the first- and second-order Doppler spectra; "flim" sets the threshold for spectral points below the peak energy; and "currmax" is the maximum current speed in the area.

First-order settings		PZUB	Default
Noise factor, "noisefact"	Header, line 15, paragraph 2	2.8	4
Smearing width, "nsm"	Header, line 11, paragraph 2	2	2
Second-order structure, "nsec"	Header, line 17, paragraph 2	1	1
First–second-order separation, "fdown"	Header, line 15, paragraph 1	3.8	7.5
Peak threshold, "flim"	Header, line 12, paragraph 1	47.9	15
Frequency window, "currmax"	Header, line 11, paragraph 1	150	150

to analyze the hourly output of a standard 25-MHz SeaSonde HF system at 100-kHz bandwidth, 512-point spectral resolution, and 2-Hz sample rate. It is coded in C language, complemented by Perl scripts, and runs in background to the acquisition software with a cron job.

The algorithm solves up to 14 Doppler lines at each location (R, θ) in the area illuminated by the radar. This limit was chosen to render the proposed methodology operational in near–real time. It also was supported by the cumulative distribution of the DV quality count (i.e., number of Doppler velocities at each sector), showing that more than 99% of the time the number of merged Doppler velocities was in the [1; 10] class (Fig. 5). If more accuracy is needed, or if the algorithm is run in offline mode, then this threshold can be easily modified to include the most appropriate threshold.

The hourly radial file often presents gaps in coverage, resulting from either ambiguities in the estimation of the DOA or the processing settings. To improve statistical significance to the radar measurements, in fact, the standard processing software requires at least two observations at each range and bearing during the measurement cycle. The SNR QA–QC methodology could be used to fill gaps in the radar coverage, provided that there is at least one measurement for each (R, θ) during the acquisition cycle, this measurement satisfies the minimum SNR quality prerequisites, and, it is assumed, that a single measurement is representative of ocean currents during the sampling time step.

The choice of using SNR values as a proxy for data quality comes from a multiyear experience with SeaSonde systems and their deployment in a wide range of environments and conditions [1995–2000, central Adriatic Sea, see Kovačević et al. (2000); 2001–06 northern Adriatic Sea, see Gačić et al. (2009), Cosoli et al. (2005, 2010), and Kovačević et al. (2004); and 2007–12 northeastern Adriatic Sea, see Cosoli et al. (2012) and Mihanović et al. (2011)]. The paired analysis of radial velocity maps and Doppler spectra usually performed as a preliminary QA–QC assessment evidenced that in the majority of the cases anomalous values were associated with poor SNR values. Nevertheless, in most of the cases these data would have not been considered as spikes when conventional quality control approaches based on threshold control and the rate of change were applied (Figs. 6a,b). In the large majority of the cases, such anomalous values were introduced in the analysis by improper choices of the first-order settings from the radar operators (Table 4). Though limited to one single point in the radar domain, comparisons with independent measurement show an improvement (higher correlation coefficients, lower rms differences; see Fig. 7 and Table 5) in the comparison metrics when the SNR QA–QC approach is adopted, that is, when the SNR value is accounted for in the calculation. A detailed investigation of the radar-to-current meter velocity differences versus SNR values of radar velocities further supports the choice. Assuming that large radar-to-current meter velocity differences represent a "spike," then the main findings can be summarized as follows:

Low SNR values (SNR < 6 dB) represent a necessary condition for a spike; that is, assuming that other sources of velocity differences are negligible and that current meter data are perfect and error free, large velocity differences are associated with poorly constrained SNR radar data. It is also true that radar currents with low SNR values do not always introduce large velocity biases or errors. Nevertheless, the SNR QA–QC methodology as a conservative choice removes from the sequence those Doppler lines that do not satisfy the more severe, range-dependent SNR threshold values. With respect to more conventional QA–QC approaches, it provides the possibility of selectively removing the Doppler lines that most likely originate the velocity error without rejecting the entire record.

However infrequently, large velocity differences can occur with high SNR–valued radar currents. This result can be interpreted in terms of ambiguities in the direction-finding algorithm. That is, ambiguities in the determination of the arrival of the sea echo that typically affects direction-finding systems, such

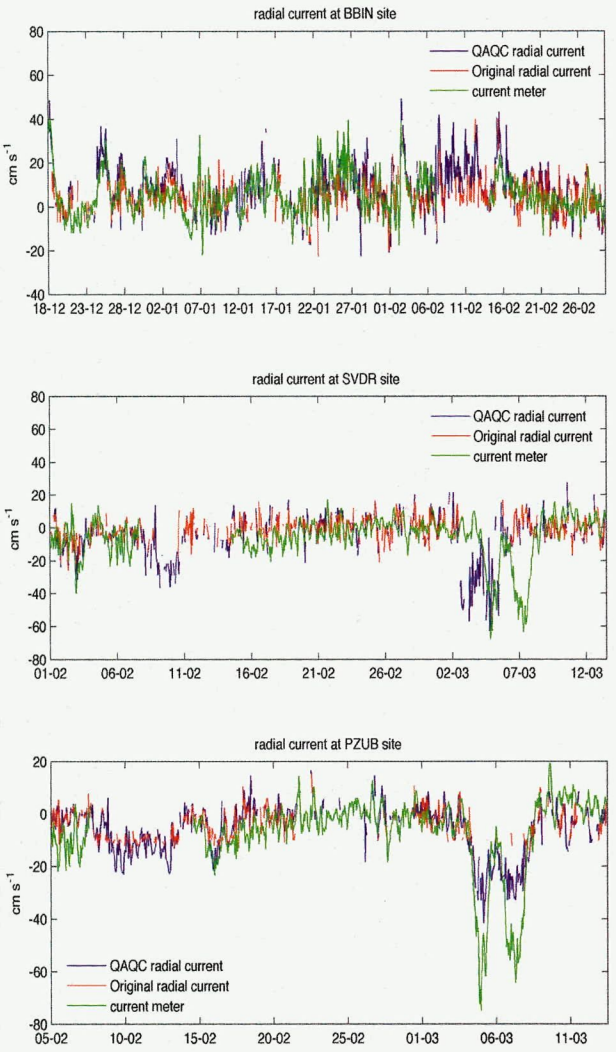

FIG. 7. Time series plot of radial velocities at the three radar sites (BBIN, SVDR, and PZUB, respectively), compared to the radial component of the subsurface currents at the MAMBO-4 buoy. The original record (red lines), the results of the SNR QA–QC analysis (blue lines), and the current meter record at the buoy (green lines) are shown.

as the SeaSonde (Paduan et al. 2006; dePaolo and Terrill 2007), are believed to place "true" ocean currents at "wrong" bearing angles. This hypothesis is currently under investigation. These inconsistent velocities are removed from the map by the consistency check in the SNR QA–QC approach.

Low SNR–valued radar velocities are common at all ranges, but their occurrence increases as range to the radar system increases. Field data for the Adriatic Sea used in our study showed a linear decrease in SNR values with ranges of approximately 1.5 dB $(1.5\ \text{km})^{-1}$ from range cells 3 to 30 (Fig. 4), coherently with the simulation approach in dePaolo and Terrill (2007).

TABLE 5. Comparison metrics (correlation coefficient and root-mean-square differences) of radial currents at the three radar stations before and after the SNR QA–QC analysis vs the current meter record at the MAMBO-4 buoy.

	Correlation		RMS differences (cm s^{-1})	
Radar site	Before SNR QA–QC	After SNR QA–QC	Before SNR QA–QC	After SNR QA–QC
PZUB	0.24	0.64	11.64	9.33
SVDR	0.14	0.18	17.36	14.82
BBIN	0.21	0.40	9.46	9.06

Though the SNR QA–QC procedure is applied to conventional monostatic acquisition geometries, its extension and implementation to bistatic and multistatic geometries is currently under investigation.

Acknowledgments. This study has been conducted through financial assistance of the European Union (INTERREG IIIa Adriatic Cross Border Programme, project NASCUM) and coordinated by the Consortium for Coordination of Research Activities Concerning the Venice Lagoon System (CORILA), Venice (Italy). Moored data were made available thanks to the Civil Protection, Friuli Venezia-Giulia (Italy) region. The manuscript benefitted from discussions with three anonymous reviewers.

REFERENCES

Barrick, D., 2002: Geometrical Dilution of Statistical Accuracy (GDOSA) in multi-static HF radar networks. SeaSonde Tech. Doc., 9 pp. [Available online at http://www.support.seasonde.com/Technician_Info/Docs/Informative/GDOSA_Definition.pdf.]

Barth, A., A. Alvera-Azcarate, K.-W. Gurgel, J. Staneva, A. Port, J.-M. Beckers, and E. V. Stanev, 2010: Ensemble perturbation smoother for optimizing tidal boundary conditions by assimilation of high-frequency radar surface currents—Application to the German Bight. *Ocean Sci.*, **6,** 161–178.

Breivik, Ø., and Ø. Sætra, 2001: Real time assimilation of radar currents into a coastal ocean model. *J. Mar. Syst.,* **28,** 161–182.

Chapman, R. D., and H. C. Graber, 1997: Validation of HF radar measurements. *Oceanography,* **10,** 76–79.

——, L. K. Shay, H. C. Graber, J. B. Edson, A. Karachintsev, C. L. Trump, and D. B. Ross, 1997: On the accuracy of HF radar surface current measurements: Intercomparisons with ship-based sensors. *J. Geophys. Res.,* **102** (C8), 18 737–18 748.

CODAR, 2005: SeaSonde 10 CrossSpectra File Format, Oct 26, 2005. 3 pp. [Available online at http://codar.com/Manuals/SeaSonde/Docs/GuidesToFileFormats/File_CrossSpectra.pdf.]

Cosoli, S., M. Gacic, and A. Mazzoldi, 2005: Comparison between HF radar current data and moored ADCP current

meter. *Nuovo Cimento,* **28C,** 865–879, doi:10.1393/ncc/i2005-10032-6.

——, A. Mazzoldi, and M. Gačić, 2010: Validation of surface current measurements in the northern Adriatic Sea from high-frequency radars. *J. Atmos. Oceanic Technol.,* **27,** 908–919.

——, M. Gačić, and A. Mazzoldi, 2012: Surface current variability and wind influence in the Northeastern Adriatic Sea as observed from high-frequency (HF) radar measurements. *Cont. Shelf Res.,* **33,** 1–13, doi:10.1016/j.csr.2011.11.008.

Crombie, D. D., 1955: Doppler spectrum of sea echo at 13.56 Mc/s. *Nature,* **175,** 681–682.

dePaolo, T., and E. Terrill, 2007: Skill assessment of resolving ocean surface current structure using compact-antenna-style HF radar and the MUSIC direction-finding algorithm. *J. Atmos. Oceanic Technol.,* **24,** 1277–1300.

Emery, B. M., L. Washburn, and J. A. Harlan, 2004: Evaluating radial current measurements from CODAR high-frequency radars with moored current meters. *J. Atmos. Oceanic Technol.,* **21,** 1259–1271.

Gačic, M., V. Kovačevic, S. Cosoli, A. Mazzoldi, J. D. Paduan, I. Mancero Mosquera, and S. Yari, 2009: Surface current patterns in front of the Venice Lagoon. *Estuarine Coastal Shelf Sci.,* **82,** 485–494, doi:10.1016/j.ecss.2009.02.012.

Goring, D. G., and V. I. Nikora, 2002: Despiking acoustic Doppler velocimeter data. *J. Hydraul. Eng.,* **128,** 117–126.

Kovačević, V., M. Gačić, I. Mancero Mosquera, A. Mazzoldi, and S. Marinetti, 2004: HF radar observations in the northern Adriatic: Surface current field in front of the Venetian lagoon. *J. Mar. Syst.,* **51,** 95–122.

——, ——, A. Mazzoldi, G. Dallaporta, and A. Gaspari, 2000: Sea-surface currents measured by coastal HF radar offshore Ancona. *Boll. Geofis. Teor. Appl.,* **41** (3–4), 339–355.

Laws, K., J. D. Paduan, and J. Vesecky, 2010: Estimation and assessment of errors related to antenna pattern distortion in CODAR SeaSonde high-frequency radar ocean current measurements. *J. Atmos. Oceanic Technol.,* **27,** 1029–1043.

Mihanović, H., S. Cosoli, I. Vilibic, D. Ivankovic, V. Dadic, and M. Gačic, 2011: Surface current patterns in the northern Adriatic extracted from high frequency radar data using self-organizing map analysis. *J. Geophys. Res.,* **116,** C08033, doi:10.1029/2011JC007104.

NOAA, 2005: Second workshop report on the quality assurance of real-time ocean data, July 2005, Norfolk, VA. CCPO Tech. Rep. Series 05-01, 48 pp.

Oke, P., J. S. Allen., R. N. Miller, G. D. Egbert, and P. M. Kosro, 2002: Assimilation of surface velocity data into a primitive equation coastal ocean model. *J. Geophys. Res.,* **107,** 3122, doi:10.1029/2000JC000511.

Paduan, J. D., and H. C. Graber, 1997: Introduction to high frequency radar: Reality and myth. *Oceanography,* **10,** 36–39.

——, and I. Shulman, 2004: HF radar data assimilation in the Monterey Bay area. *J. Geophys. Res.,* **109,** C07S09, doi:10.1029/2003JC001949.

——, P. M. Kosro, and S. M. Glenn, 2004: A national coastal ocean surface current mapping system for the United States. *Mar. Technol. Soc. J.,* **38,** 102–108.

——, K. C. Kim, M. S. Cook, and F. P. Chavez, 2006: Calibration and validation of direction-finding high-frequency radar ocean surface current observations. *IEEE J. Oceanic Eng.,* **31,** 862–875, doi:10.1109/JOE.2006.886195.

Parks, A. B., L. K. Shay, W. E. Johns, J. Martinez-Pedraja, and K.-W. Gurgel, 2009: HF radar observations of small-scale surface current variability in the Straits of Florida. *J. Geophys. Res.,* **114,** C082002, doi:10.1029/2008JC005025.

Schmidt, R. O., 1986: Multiple emitter location and signal parameter estimation. *IEEE Trans. Antennas Propag.,* **34,** 276–280.

Shulman, I., C.-R. Wu, J. K. Lewis, J. D. Paduan, L. K. Rosenfeld, J. C. Kindle, S. R. Ramp, and C. A. Collins, 2002: High resolution modeling and data assimilation in the Monterey Bay area. *Cont. Shelf Res.,* **22,** 1129–1151.

Stewart, R. H., and J. W. Joy, 1974: HF radio measurement of surface currents. *Deep-Sea Res.,* **21,** 1039–1049.